Application of Graphitic Bio-Carbon using Two-Level Factorial Design for Microwave-assisted Carbonization

Zaira Z. Chowdhury, Wageeh A. Yehye,[a,*] Nurhidayatullaili Muhd Julkapli,[a] Mohammed Abdul Hakim Al Saadi,[a] Mautaz Ali Atieh,[b]

A novel intermittent microwave-assisted carbonization method was developed to prepare bio-char (BWSC) from Durian wood sawdust (BWS). The BWS was further activated using a base-catalytic approach to produce a graphitic form of bio-carbon (BWSAC). A three factor, two-level central composite (CCD) experimental design was used to maximize Pb(II) ion removal from aqueous solution using BWSAC. Three independent variables (initial pH of solution (pH_0) ranging from 2 to 8, initial metal ion concentration of Pb(II) cations (C_0) ranging from 50 to 100 mg/L, and contact time (C_t) ranging from 10 to 300 min) were consecutively coded as x_1, x_2, and x_3 at three levels (−1, 0 and 1) of the design matrix. The experimental conditions in terms of actual factors were determined to be x_1 (pH_0) = 5.86, x_2 (C_0) = 57.77 mg/L, and x_3 (temperature) = 53.85 °C, and the resultant Pb(II) ion removal efficiency (y_1) obtained was 92.73%, with a model desirability of 0.974. The change in physiochemical properties after carbonization as well as activation was observed by scanning electron microscopy (SEM), X-ray diffraction (XRD), Brunauer, Emmett and Teller surface area analysis (BET), Thermogravimetric analysis (TGA), Ultimate analysis, and Fourier transform infrared spectroscopy (FTIR) .

Keywords: Biomass; Graphitic carbon; Central composite design; Response surface methodology

Contact information: a: Nanotechnology and Catalysis Research Center (NANOCAT), IPS Building, University Malaya, Kuala Lumpur 50603, Malaysia; b: Qatar Environment and Energy Research Institute, Qatar Foundation, PO Box 5825, Doha, Qatar;
** Corresponding author: wdabdoub@um.edu.my*

INTRODUCTION

The impending scarcity of non-renewable fossil fuels has led to the consideration of waste lignocellulosic biomass to produce biocarbon for waste water treatment. Thus, biomass can be regarded as one of the most expedient precursors to obtain carbon-rich materials. Preparation of bio-chemicals from lignocellulosic residues is a grand challenge of our time (Kobayashi *et al.* 2016).

Increasing attention is being given to the imminent health hazards caused by careless discarding of heavy metals into the aquatic environment (Chowdhury *et al.* 2012a). Mining and metallurgical waste waters are the major sources of heavy metal accumulation in the environment. Thus, the elimination of metal ions from waste streams has resulted in the expansion of new, cost-effective separation technologies.

Conversion of lignocellulosic residues for synthesis of activated char and adsorption of metallic pollutants from aqueous effluents is regarded as a useful substitute compared with conventional separation techniques (such as precipitation, coagulation, oxidation, electrochemical processes, and/or membrane processes) (Veglio and Beolchini 1997). Most of these conventional methods are often ineffective when the heavy metal

ion concentration is in the range of 10 to 100 mg/L, and the permissible limit is less than 1 mg/L (Holan and Volesky 1994). In this context, the adsorption of metal ions onto activated char is considered an innovative approach. This method is inexpensive as well as competitive, and it has been shown to be more effective than various alternative measures (Volesky *et al.* 1992; Ucun *et al.* 2002). Adsorption is considered an ecofriendly, versatile treatment and is extensively used for the disposal of waste effluent and toxic gas elimination from air in process industries. The effectiveness of the adsorption process lies in the simplicity of process design, economic feasibility, and reuse of potential adsorbents for recycling and long-term applications. Adsorption using biomass-derived char has been ascertained to be the least expensive technique, especially for treating wastewater streams of low metal ion concentrations as well as maintaining the rigorous treatment of metallic pollutants in drinking water (Sahu *et al.* 2009a).

Among the metallic pollutants, lead is extremely toxic for living organisms, even at low concentrations. Metallic lead is used for storage batteries, fertilizers, pesticides, printing processes, dyes and pigments, fuels, and explosives (Jalali *et al.* 2002). It can cause damage to the nervous system, gastrointestinal track, kidneys, and reproductive system, predominantly in children (Feng *et al.* 2004). It can cause diseases like anemia, encephalopathy, hepatitis, and nephritic syndrome (Lo *et al.* 1999). Previous studies have reported that moderate poisoning from lead(II) cation exposure can result in neurobehavioral and intelligence discrepancies in humans (Selatnia *et al.* 2004; Chen *et al*. 2007).

Graphitic carbon materials with micro- and mesoporous textures and high surface area have attracted attention because of their potential application in super-capacitors, field emission, catalyst support, adsorption, and solar energy conversion (Kumar *et al.* 2012). With respect to the subtle electronic properties, antifouling properties, and ability to promote electron transfer reactions, graphitic carbon materials also find interesting application in biosensoring devices. In addition, because of their bioselectivity for redox enzymes, these materials have proven to be very useful for the quantification of various organic substances, including glucose (Lu *et al.* 2007), protein (Avramescu *et al.* 2002), DNA, pesticides (Daniel *et al.* 1997), and hydroquinone (Vieira and Fatibello-Filho 2000). Synthesis of graphitic biocarbon materials requires additional high-temperature treatment (Kumar *et al.* 2012). Microwave-assisted pretreatment offers the apparent advantage of carbonization of biomass at comparatively lower temperature and time, which is energy-efficient. It has been reported that microwave-assisted pre- and post-heating is a very effective method for modifying the surface chemistry of carbon fiber (Sathish-Kumar *et al.* 2012). Biocarbon is a black, non-toxic, solid carbonaceous material primarily derived from agricultural residues resembling a granular or powder form of charcoal (Chowdhury *et al.* 2013). With activation, its properties can be easily changed to have large internal surface area and porosity with high mechanical strength (Chowdhury *et al.* 2012b). Activated biochar- or biocarbon-based systems can remove a large variety of toxic pollutants from the solution phase with very high efficiencies (Liu and Zhang 2009; Han *et al.* 2013; Singanan and Peters 2013; Zhu *et al.* 2013; Mohan *et al.* 2014). Numerous attempts have been made to prepare biocarbon from lignocellulosic waste (Antal *et al.* 2007; Funke and Ziegler 2010; Jamari and Howse 2012). Recently, tamarind wood (Singh *et al.* 2008), digested sewage sludge and coconut husk (Tay *et al.* 2001), palm shell (Adinata *et al.* 2007), rice husk (Sahu *et al.* 2009b), rubber wood sawdust (Srinivasakannan and Bakar 2004), bamboo waste (Ahmad and Hameed 2010), and rattan

sawdust (Ahmad *et al.* 2009) have been utilized as low-cost feedstocks to obtain biocarbon with unique properties.

In this work, biochar was synthesized from Durian wood based sawdust (BWS) using a two-step microwave-assisted semi-carbonization and physio-chemical activation method. The prepared char sample (BWSC) was further activated to obtain mesoporous-structured graphitic carbon because liquid-phase adsorption is mainly dominated by mesopores. Durian (*Durio zibethinus*) is a kind of tropical fruit that is abundant in South East Asia. It belongs to the family Bombaceae and genus *Durio* (Jun *et al.* 2010). It is well-known as the "King of Fruits". Malaysia produces *Durio zibethinus* commercially, and the annual production of durian in Malaysia was approximately 376,273 metric tons in the year 2008 (Department of Agriculture Malaysia 2009). There has been no research on the synthesis of bio-char from Durian wood sawdust using microwave-assisted carbonization and its subsequent activation for waste water treatment. The conventional method for analyzing a synthetic process, keeping other factors at an unstipulated persistent level, does not illustrate the combined effects of all the variables involved. In that case, the optimization process of a multivariable system typically outlines one factor at a time. This method involves a lot of experiments to be performed, and even then, it cannot disclose the interaction effects between the factors involved. This makes the overall process time-consuming, as it requires a large number of experiments to define optimum levels, which are not reliable enough for process design. Recently, several types of statistical investigational design methods have been developed for chemical process optimization. Experimental design method is a very advantageous contrivance for this purpose. It delivers mathematical models, which are helpful in explicating the interactions among the parameters under consideration (Alam *et al.* 2007). Among these methods, response surface methodology (RSM) is one of the most appropriate methods employed in many fields. The RSM technique is a collection of mathematical and statistical methods that is useful for developing, improving, and optimizing processes and can be employed to appraise the relative importance of numerous affecting factors, even in complex interactions. The purpose of using RSM is to define the optimum operational conditions for the system or to limit a region that contains the operating stipulations (Montgomery 2001). In this work, the influence of several operating parameters, *i.e.*, initial concentration, temperature, and pH, were studied in batch mode using the activated biocarbon sample (BWSAC). The optimum values of the selected variables were determined by resolving the quadratic regression model, as well as by interpretation of the response surface contour plots.

EXPERIMENTAL

Materials

The starting sawdust sample of BWS derived from Durian wood was collected from a local sawmill in Penang, Malaysia. The sawdust was ground and sieved. The average particle size of the sieved biomass sample was kept at approximately 0.2 to 0.4 mm. The ground BWS sample was washed with deionized water and then dried at 110 °C for 24 h. It was stored in a sealed container for preliminary characterization. Hydrochloric acid (HCl) and potassium hydroxide (KOH) pellets were purchased from Sigma Aldrich, Malaysia. The chemicals purchased were of analytical grade.

Methods

Microwave-assisted carbonization of biomass wood sawdust (BWS)

The dried biomass sample was carbonized using deionized water under microwave irradiation (Ethos Plus, Millestone, USA), where the biomass to solvent ratio was kept at 1:25 (based on dry weight of biomass). One gram of biomass sample was added with 25 mL deionized water in 70 mL autoclave tube and placed inside the microwave for char synthesis. During the microwave-assisted carbonization process, the sample was irradiated at 2.45 GHz, and the power was kept at 750 W. The sample was carbonized for 60 min at a temperature of 220 °C under nitrogen flow. The char thus obtained was filtered and labeled BWSC. The BWSC sample was washed several times with hot deionized water. The sample was oven-dried at 50 °C and stored in an air-tight container for further characterization.

Fixed bed pyrolysis of biochar (BWSC)

The prepared biochar (BWSC) was impregnated with solid KOH pellets. The ratio between BWSC and solid KOH was kept at 1:0.5 (based on weight), which means that 100 g of char sample was mixed with 50 gram of KOH pellets. Approximately 500 mL of deionized water was added to the impregnated BWSC sample with constant stirring. The mixture with KOH pellets was then heated at 90 to 100 °C for 6 h to ensure the unclogging of pores as well as disruption of residual lignocellulosic linkages, with subsequent removal of partially burnt debris materials from the surface. The mixture was kept overnight in an oven at 105 °C to dry the sample completely. To enhance the surface area of the final product, it was further pyrolyzed in presence of carbon dioxide gas flow at 700 °C for 2 h and labeled BWSAC. KOH and CO_2 gas flow were used as chemical and physical activating agent, respectively.

Multivariable design of experiment

In this work a central composite design (CCD) was applied to study the variables for adsorption of Pb(II) cations from aqueous solution using BWSAC in a batch process. The design CCD is extensively used for fitting an empirical second-order polynomial equation. Usually, CCD is based on 2n factorial runs, with 2n axial runs and nc center runs (six replicates). For two-level factorial designs, each variable is investigated at two levels. However, as the number of factors, n, increases, the number of runs for a complete replicate of the design also increases. The response of removal percentage (y_1) and the corresponding factors were modeled and optimized by ANOVA. This helps to estimate the statistical parameters governing the sorption process. Overall, the optimization process contains three major steps: statistically designing and performing the experiments, determining the coefficients in a mathematical model, and analyzing the adequacy of the model according to Eq. 1,

$$Y = f(X_1, X_2, X_3, X_4 - - - - - X_n) \quad (1)$$

where Y is the response of the system and X_i is the variable under investigation for the process. The goal is to optimize the response variable (Y). Table 1 summarizes the range of variables in terms of actual and coded factors.

Table 1. Independent Variables for Pb(II) Adsorption with their Actual and Coded Levels

Variables	Code	Units	Coded Variable Levels				
			-α	-1	0	+1	+α
pH	x_1	-	0.45	2.50	5.50	8.50	10.55
Concentration	x_2	mg/L	32.96	50.00	75.00	100.00	117.06
Temperature	x_3	°C	19.77	30.00	45.00	60.00	70.23

It is expected that the independent variables are continuous and manageable by experiments with insignificant errors. The goal is to find an appropriate estimate for the accurate functional relationship between independent variables and the response surface (Gunaraj and Murugan 1999). The order of experimental runs was randomized to minimize the effects of the uncontrolled factors. The response obtained was used to develop an empirical model that correlated the response of adsorption uptake of lead ions from a single solute system using a second-degree polynomial equation, given by Eq. 2,

$$Y = b_0 + \sum_{i=1}^{n} b_1 x_1 + \sum_{i=1}^{n} b_{11} x_i^2 + \sum_{i=1}^{n} \sum_{j>1}^{n} b_{ij} x_i x_j \quad (2)$$

where Y is the predicted response, b_0 is the constant coefficient, b_1 is the linear coefficient, b_{ij} are the interaction coefficients, b_{ii} are the quadratic coefficients, and x_i, x_j are the coded values of the adsorption. For three variables, the recommended number of tests at the center point is six. Hence, the total number of tests (N) required for the three independent variables is:

$$N = 2n + 2n + nc = 2 \times 3 + (2 \times 4) + 6 = 20 \quad (3)$$

Once the desired ranges of values of the factors are predetermined, they are coded to lie at ±1 for the factorial points, 0 for the center points, and ± α for the axial points. The complete layout for the design matrix is provided by Table 2.

Batch adsorption study

An aqueous Pb(II) solution having an ion concentration of 1000 mg/L was prepared. A known amount of corresponding lead nitrate salt was dissolved in 1 L of distilled water to obtain stock solution. The stock solution thus obtained was diluted as required to obtain standard solutions of concentrations provided by the basic design matrix (Table 2).

The experiments were performed in a thermal water bath shaker at various temperatures for a predetermined period of time at 150 rpm using 250-mL Erlenmeyer flasks containing (50 ± 0.2) mL of various concentrations of Pb(II) ions solutions with 0.2 g of BWSAC, with the pH, concentration, and temperature levels defined by Table 2. Preliminary screening studies showed that the system reached equilibrium within 6 h; after that, the uptake percentage varied insignificantly. Thus the samples were taken out after 6 h and the residual concentration in the solution was analyzed using atomic absorption spectroscopy (AAS) (Perkin-Elmer-6000, Germany) after filtering the activated BWSAC sample.

Table 2. Central Composite Design and Experimental Responses for Adsorption Percentage onto BWSAC

Sample ID	Run	Type of Point	Level (coded Factors)			Reaction Variables (Actual Factors)			Percentage Removal (observed)
						pH x_1	Concentration x_2 (mg/L)	Temperature x_3 (°C)	y_1
S-1	1	Fact	-1	-1	-1	2.50	50.00	30.00	43.98
S-2	2	Fact	+1	-1	-1	8.50	50.00	30.00	46.99
S-3	3	Fact	-1	+1	-1	2.50	100.00	30.00	29.99
S-4	4	Fact	+1	+1	-1	8.50	100.00	30.00	39.88
S-5	5	Fact	-1	-1	+1	2.50	50.00	60.00	51.88
S-6	6	Fact	+1	-1	+1	8.50	50.00	60.00	65.98
S-7	7	Fact	-1	+1	+1	2.50	100.00	60.00	39.88
S-8	8	Fact	+1	+1	+1	8.50	100.00	60.00	55.89
S-9	9	Axial	-1.681	0	0	0.45	75.00	45.00	19.99
S-10	10	Axial	+1.681	0	0	10.55	75.00	45.00	36.09
S-11	11	Axial	0	-1.681	0	5.50	32.96	45.00	94.66
S-12	12	Axial	0	+1.681	0	5.50	117.04	45.00	63.99
S-13	13	Axial	0	0	-1.681	5.50	75.00	19.77	48.88
S-14	14	Axial	0	0	+1.681	5.50	75.00	70.23	92.22
S-15	15	Center	0	0	0	5.50	75.00	45.00	86.55
S-16	16	Center	0	0	0	5.50	75.00	45.00	87.33
S-17	17	Center	0	0	0	5.50	75.00	45.00	86.44
S-18	18	Center	0	0	0	5.50	75.00	45.00	86.23
S-19	19	Center	0	0	0	5.50	75.00	45.00	87.99
S-20	20	Center	0	0	0	5.50	75.00	45.00	87.24

The percentage removal of Pb(II) ions was calculated according to Eq. 4,

$$\%removal = \frac{C_0 - C_e}{C_0} \times 100 \quad (4)$$

where C_0 and C_e are the initial and equilibrium concentrations (mg/L) of Pb(II) ions in the solution, respectively.

Physicochemical characterization

The changes in the morphologies of BWS, BWSC, and BWSAC were observed using a scanning electron microscope (SEM, Model Leo Supra 50VP Field Emission, UK). The crystalline structure of the samples was analyzed using X-ray diffraction (XRD, Burker AXSD8 Avance, Germany) at 40 kV and 40 mA using Cu-Kα radiation sources. Thermogravimetric analysis coupled with a differential thermal analyzer (DTA) (Mettler Toledo Star SW901, Japan) was carried out to determine the thermal stability of the samples under a 5 mL/min nitrogen flow. In the TGA analysis, 7 mg of each sample was heated under a N_2 flow at 1000 °C with a heating rate of 5 °C/min. The BET surface area, pore volume, and pore size distribution of BWS, BWSC, and BWSAC were analyzed with an Autosorb 1, Quantachrome Autosorb automated gas sorption system supplied by Quantachrome, Japan. The samples were outgassed under vacuum at 400 °C for 4 h to remove moisture content before nitrogen gas adsorption. The changes in the chemical functional groups were verified using the infrared spectroscopy technique. The FTIR spectra for BWS, BWSC, and BWSAC were recorded using a Bruker spectrometer model IFS 66V/S (USA). The FT-IR spectra were recorded in the range of 400 to 4000 cm^{-1}.

RESULTS AND DISCUSSION

Experimental Design and Fitting of Mathematical Model

The results obtained for each trial conducted as per the experimental design matrix are given in Table 2. The solicitation of the response surface methodology for the estimated parameters indicated an empirical relationship between the response and input factors, which is illustrated by the following quadratic model (Eq. 5), where y_1 represents the removal percentage:

$$y_1 = 87.31 + 5.14x_1 - 6.96x_2 + 9.10x_3 + 1.10x_2 + 2.15x_1x_3 - 0.12x_2x_3 - 2312x_1^2 - 498x_2^2 - 8.09x_3^2 \quad (5)$$

The linear coefficients for the variables pH (x_1), concentration (x_2), and temperature (x_3) demonstrate the effect of that individual variable on Pb(II) ion uptake from water by BWSAC. The constants shown as the product of two variables, namely x_1x_2, x_2x_3, and x_3x_1, illustrate the collective impact on those responses. x_1^2, x_2^2, and x_3^2 denote quadratic results. A positive sign in front of the equation is an indication of the synergistic influence, whereas a negative sign indicates an incompatible influence of process factors on responses. The significance of each parameter shown in Eq. 5 was determined by the p-values (Montgomery 2001). The results obtained for the quadratic model for percentage adsorption (y_1) in terms of ANOVA are provided in Table 3. The values of R^2 and adjusted R^2 are near 1.0 (Table 4), which suggests a high correlation

between the observed and predicted values. This means that the proposed model delivers an excellent interpretation of the relationship between the independent variables (factors) and the response, y_1.

Table 3. ANOVA Analysis and Lack of Fit Test for Quadratic Modeling of Removal Percentage of Pb(II) Ions from Synthetic Waste Water by BWSAC

Source	Sum of Squares	Degree of Freedom	Mean Square	F Value	Prob> F	Comments
Model	10477.91	9	1164.21	20.90	<0.0001	*Significant*
x_1	359.69	1	359.69	6.46	0.0293	
x_2	657.65	1	657.65	11.81	0.0064	
x_3	1156.58	1	1156.58	20.76	0.0010	
x_1x_2	9.66	1	9.66	0.17	0.6859	
x_1x_3	37.02	1	37.02	0.66	0.4339	
x_2x_3	0.12	1	0.12	0.002	0.9635	
x_1^2	7700.34	1	7700.34	138.23	<0.0001	
x_2^2	357.91	1	357.91	6.42	0.0296	
x_3^3	942.25	1	942.25	16.91	0.0021	
Residuals	557.08	10	55.71			
Lack of Fit	554.83	5	110.97	246.86	<0.0001	*Significant*
Pure Error	2.25	5	0.45			

The value for Prob > F obtained for the model is lower than 0.05 (*i.e.*, a = 0.05, or 95% confidence), which indicated that the model is statistically significant. Investigation of the fit summary output illustrated by Table 3 revealed that the quadratic model is statistically significant for the desired response. Hence, it can used for further analysis. For the response of removal percentage, y_1, pH (x_1), and concentration (x_2) had more moderate influences than temperature (x_3), *i.e.*, temperature had the greatest influence on removal percentage. The interaction influences of pH and concentration (x_1x_2) and pH and temperature (x_1x_3) were more prominent than the other interaction factor (x_2x_3) related to the percentage removal, y_1. In this case, x_1, x_2, and x_3 and their quadratic terms are significant.

Table 4. Statistical Parameters for Model Verification

Statistical Parameters	**% Removal**
	***y*₁**
Standard Deviation, SD%	7.46
Correlation Coefficient, R^2	0.949
Adjusted R^2	0.904
Mean	62.60
Coefficient of Variation, CV	11.92
Adequate Precision	14.02

From Table 4, it can be observed that the experimental R^2 value was in reasonable agreement with the adjusted R^2. The values obtained for co-efficient of variation (CV) and standard deviation were small, suggesting the reproducibility of the model. The values of adequate precision were determined based on signal-to-noise ratio. For effective model simulation, the adequate precision should be larger than 4. The adequate precision observed for y_1 was 14.02. This revealed that the experimental data obtained here are statistically significant to prepare the design matrix of Table 2.

Figure 1 shows the linear plot of predicted *versus* experimental percentage removal of Pb(II) cations (y_1) by BWSAC. As can be observed from this plot, the predicted values for the percentage removal were legitimately close to their experimental values. The R^2 value for Eq. 5 was 0.949, which was near to unity, reflecting the suitability of the model.

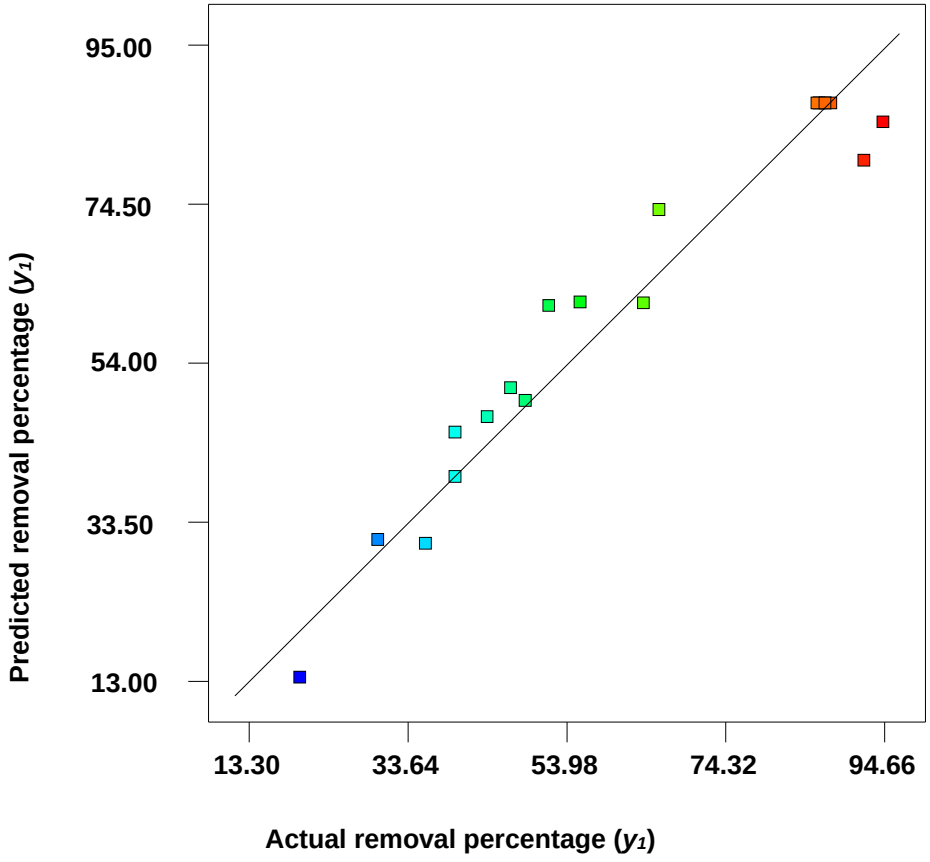

Fig. 1. Predicted *versus* actual percentage removal of Pb (II) cations using BWSAC

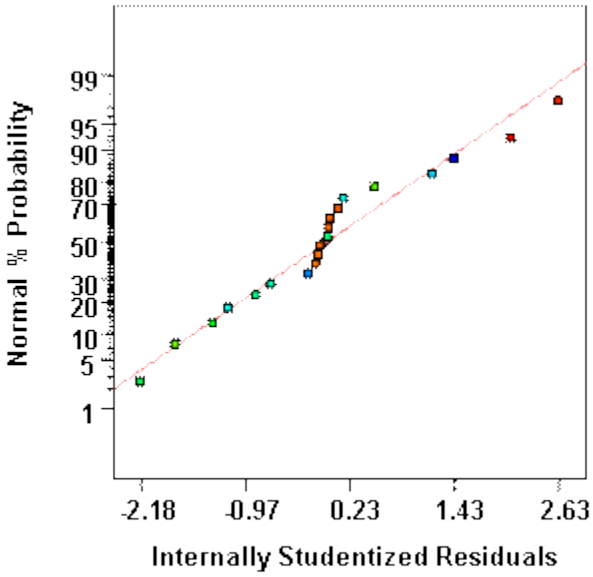

Fig. 2. Normal probability plot for percentage removal of Pb (II) cations using BWSAC

Analysis of Residual Graphs

The normality of the experimental points can be checked by plotting the normal probability plot of the residuals for percentage removal for Pb(II) cations onto BWSAC. The normal probability plot is a graphical illustration for quantifying whether or not a data set is approximately normally scattered. The residual reflects the difference between the observed and the predicted value (or the fitted value) from the regression. If the data points on the plot are reasonably close to the straight line, then the data are expected to be normally distributed. Figure 2 shows the normal probability plot of residual values. The experimental points are reasonably associated with the straight line, signifying a normal distribution. Since the adsorption data points on the plot are scattered legitimately adjacent with the straight line, it is expected that the data are normally distributed (Abd Hamid *et al*. 2014).

Figure 3(a) shows Studentized residuals *versus* the fitted value whereas Fig. 3(b) shows Studentized residuals *versus* experimental runs for the percentage removal. The data points for residuals are randomly scattered about zero. This demonstrates that the variance of experimental observations is constant. All of the data points observed are found to fall within the range of +3 to -3. This confirms that no response transformation is needed for the experimental design of this study.

To investigate the interactive effect of two factors on the percentage removal of the Pb(II) ions, three-dimensional (3D) response surfaces with contour plots were drawn. The inferences obtained from those plots are discussed below.

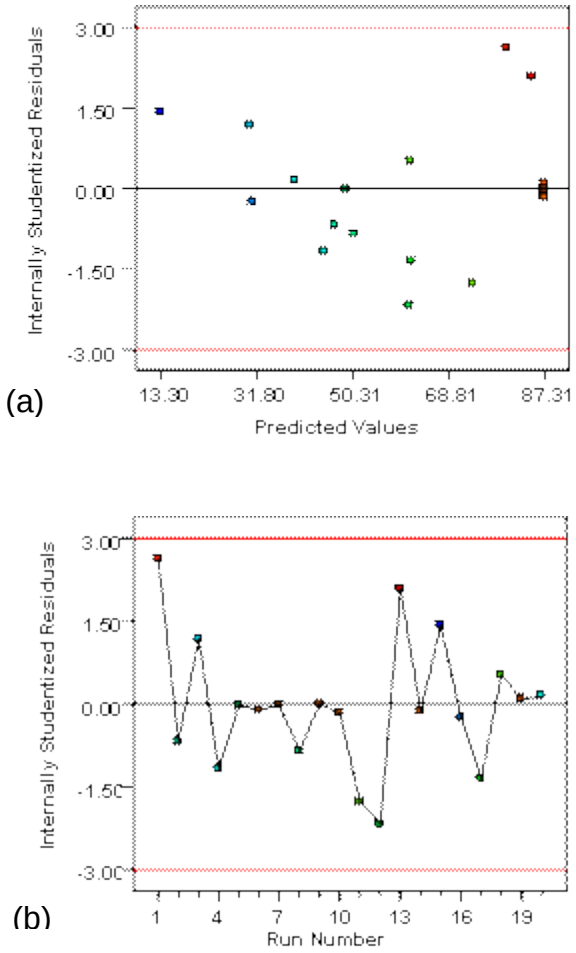

Fig. 3. (a) Studentized residuals *versus* fitted plot and (b) studentized residuals *versus* run number for removal percentage of Pb(II) cations onto BWSAC

Interpretation of Response Surface Contour Plots

A response surface is the prediction of a contour plot as a 3D plane. To investigate the interactive effect of two factors on the percentage removal of the Pb(II) ions, 3D response surfaces with contour plots were drawn. The inferences thus obtained are discussed below. In this case, two variables were changed, but the third variable was set to its center value. Figure 4a shows a 3D response surface plot of the combined effect of pH and initial Pb(II) ion concentration on removal percentage. It is clear from the figure that the removal percentage increased with increasing pH up to 6.0, after which it decreased. It was also observed that removal percentage decreased with increasing metal ion concentration. At higher concentrations, there are more ions competing to be adsorbed; therefore, less removal efficiency was observed.

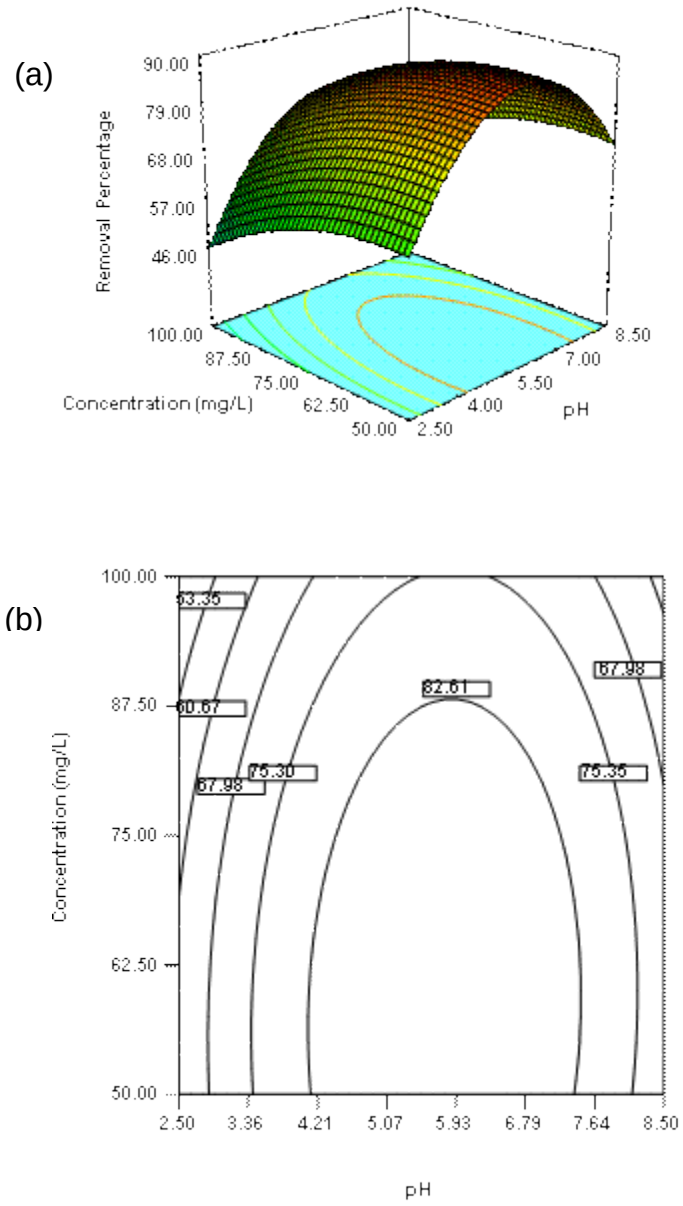

Fig. 4. (a) Response surface and (b) contour plots of the combined effects of pH (x_1) and initial concentration (x_2) when temperature (x_3) is at its center point

When the solution pH was lower than 4, the removal percentage was low because of competition between positive hydrogen and metal ions at the binding sites of the prepared carbon (Pavan *et al.* 2008). A relatively strong interaction between initial concentration and pH was reflected by the elliptical nature of the contour curve (Fig. 4b). It showed an increase in Pb(II) ion removal percentage from 53.35 to 82.61 (Fig. 4b). Thus, a combination of higher initial concentration and moderate range of pH can result in the maximum lead removal percentage. The metal solubility seemed to decrease at higher pH, and precipitation started to decrease the removal percentage at pH 8.5 (Yan and Viraraghavan 2003). At higher pH, precipitation of Pb(II) cations can block the pores of carbon, resulting in lower removal efficiency (Yan and Viraraghavan 2003).

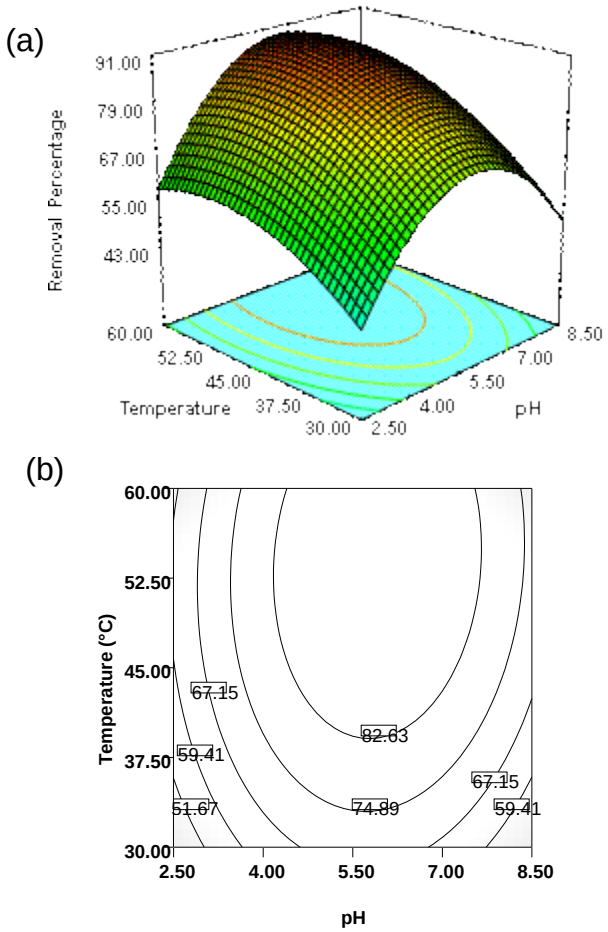

Fig. 5. (a) Response surface and (b) contour plots of the combined effects of pH (x_1) and temperature (x_3) when initial concentration (x_2) is at its center point

Figure 5 shows the combined effect of pH and temperature on the removal percentage of lead. The curve reveals that the removal percentage increased with increasing temperature (Fig. 5a). The robust interaction effect of pH and temperature can be illustrated by a circular contour plot (Fig. 5b). The increase in lead uptake with increasing temperature reflects the endothermic nature of sorption.

Alternatively, these effects might be attributed to the higher rate of diffusion of the pollutant species across the external boundary layer as well as inside the pores of the carbon particle with increasing temperature. Increasing temperature might decrease the viscosity of the solution (Wang and Zhu 2007). It has been reported that the active surface sites increase proportionally with increasing temperature to enhance the uptake capacity of the pollutant species (Bulut and Tez 2007).

Process Optimization

For successful adsorption process design, relatively high removal efficiencies are expected for targeted pollutants under optimum condition. As observed from the basic design matrix, when pH and temperature increased, the percentage ion removal increased up to a certain limit, whereas concentration had the opposite effect. To optimize the adsorption process, the targeted goal was set at maximum values for removal percentage, while the values of the three variables (pH, concentration, and temperature) were adjusted

in the ranges under study. A weight can be assigned as 1 for each goal to regulate the form of its precise desirability function. The goals were combined into an overall desirability function. Desirability is an impartial function that ranges from zero, outside of the limits, to one, at the goal (Amini *et al.* 2008). The desirability ramp for optimization is provided by Fig. 6. The error was also evaluated, as shown in Table 5.

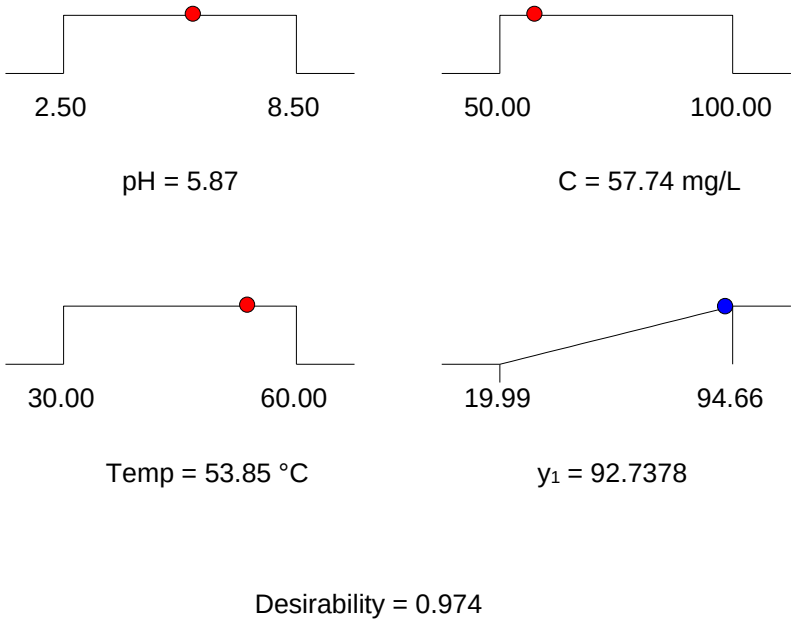

Fig. 6. Desirability ramp for numerical optimization of pH, initial concentration, temperature, and Pb(II) ion removal

Table 5. Numerical Optimization for Adsorption Percentage onto BWSAC

pH (x_1)	Concentration (x_2)	Temperature (x_3)	Percentage Removal (y_1)			Desirability
	(mg/L)	(°C)	Predicted	Experimental	Error	
5.86	57.77	53.85	92.74	91.22	1.63	0.974

Physiochemical Characterization

The surface morphological features of BWS, BWSC, and BWSAC were observed by SEM and are illustrated in Fig. 7. The outer surface of BWS was comparatively smooth, with some minor folding. Woody biomass contains cellulose, hemicellulose, and lignin, with some pectin and wax. Lignin and hemicellulose helps to bind the cellulosic fiber in bundles, which makes their surface even, with less folding and cracks, as shown by Fig. 7(a). After microwave-assisted carbonization, the surface of BWSC was still smooth, with minor amount of circular pores (Fig. 7(b)). Small amount of debris were blocking the pores which might be due to dissolution of hemicellulose and lignin partially (Zhang *et al.* 2014). However after KOH treatment and activation using carbon dioxide gas flow, a large amount of irregular pores were visible on the surfaces of the activated BWSAC (Fig. 7(c)). This implies that char formation using microwave heating with a supplementary stage of activation with KOH can competently improve the pore volume

up to a greater scale, which can subsequently increase the surface area with greater removal efficiency. This observation is further supported by BET analysis.

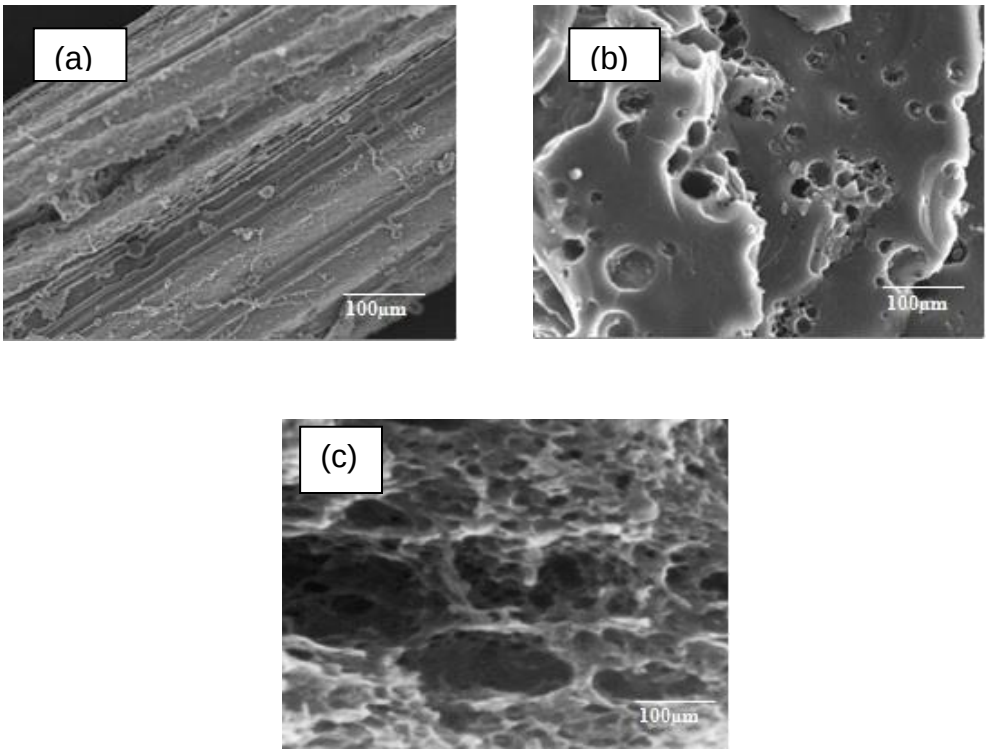

Fig. 7. SEM images of (a) BWS, (b) BWSC, and (c) BWSAC

The BET surface area and micropore surface areas of BWSC and BWSAC are provided in Table 6. The surface area of the biochar substantially increased after base catalytic treatment and the subsequent activation process. The average pore diameter of the activated char was 21.22 nm.

Table 6. Physico-Chemical Characteristics of BWSC and BWSAC

Sample Properties	BWSC	BWSAC
BET surface area	12.01 m^2/g	862.05 m^2/g
Micropore Surface area	1.20 m^2/g	1084.30 m^2/g
Total pore volume	0.1123 cc/g	0.6785 cc/g
Average pore diameter	2.01 nm	21.22 nm
BJH cumulative adsorption surface area	1.32 m^2/g	532.72 m^2/g

The surface functional groups, especially oxygen-containing groups, play a vital role in forming surface complexes with pollutant molecules, thereby initiating removal from waste water (Johari *et al*. 2013). All samples were analyzed using FTIR. The FTIR

analysis illustrates the changes in the surface functional groups of the sample with carbonization and pyrolysis. The FTIR peaks obtained for BWS, BWSC, and BWSAC are listed in Table 7. In the region of 3400 to 3600 cm^{-1}, the spectra all show broad and strong bands because of the vibration of hydroxyl groups and the stretched vibration of adsorbed water molecules (Chowdhury *et al.* 2015). This implies that after carbonization and activation, the hydroxyl groups remained in the samples. The spectra also contain an aliphatic C-H band near 2800 to 3000 cm^{-1}, which can be attributed to aliphatic stretching vibrations. The peak near the 1000 to 1400 cm^{-1} region represents C-O stretching in hydroxyl, ester, or ether, and O-H bending vibrations. The stretching vibration of C=O groups can be identified near 1450 to 1550 cm^{-1}. Minor peaks near 450 to 950 cm^{-1} can be assigned to C-H out-of plane bending vibration and O-H stretching vibrations of C-O-H bands.

Table 7. List of FTIR Peaks Observed for BWS, BWSC, and BWSAC

IR Peaks	Frequency (cm^{-1})			Peak Assignment
	BWS	BWSC	BWSAC	
1	-	-	477.53	C-H out-of-plane bending of benzene derivatives
2	-	509.79	501.03	C-H out-of-plane bending of benzene derivatives
3	604.41	602.24	-	C-O-H
4	-	-	790.12	C-H
5	835.10	839.68	-	C-H
6	907.89	-	-	O-H bending
7	1158.88	1110.82	1195.95	-C-N stretching
8	1257.76	-	-	C-O stretching
9	-	1376.77	-	CH_3 deformation
10	1411.00	1422.06	1493.33	In-plane OH bending and C-O stretch of dimmers
11	1507.32	1593.99	-	C=C ring stretching of benzene derivatives
12	1603.33	1656.45	-	C=O stretching
13	1755.97	1793.98	-	C=O stretching
14	-	-	2428.16	C=C stretching vibration of ketones, aldehydes or carboxylic group
15	-	2677.68	-	C=C stretching vibration of ketones, aldehydes or carboxylic group
16	2828.98	2852.90	-	C-H stretching
17	3403.56	3556.44	3690.07	O-H stretching vibration of hydroxyl functional groups

X-ray diffraction studies of BWS, BWSC, and BWSAC were conducted to investigate the crystalline behavior of these samples. However, no remarkable variations were observed in the appearance of the XRD patterns for the BWS, BWSC, and BWSAC. This result was expected because the activation temperature used here was below 900 °C (Acharya *et al.* 2009; Liu and Zhao 2012). A similar phenomenon was

reported during the preparation of activated char from tamarind wood and seed biomass (Sahu *et al.* 2008; Munusamy *et al.* 2011). Two diffraction peaks, at approximately 23.7^0 to 25.6^o and 41.41^o to 43.54^o, were observed for BWSC and BWSAC, corresponding to the 002 and 101 planes of the disordered hexagonal graphitic structure of carbon. The broad peaks show the amorphous nature of the prepared carbon sample (Munusamy *et al.* 2011). This suggests that the crystalline structures of the prepared biochar and activated biochar remain unchanged after treatment with KOH and activation. A similar XRD pattern was observed for cashew nut shell-based activated carbon (Tangjuank *et al.* 2009). This type of structure is known as turbostratic and can be caused by two-dimensional parallel orientation of carbon layer planes (Azargohar and Dalai 2006). The crystalline behavior of the samples are given in Table 8.

Table 8. Crystalline Structures of BWSC and BWSAC Samples

Sample	d_{002} (nm)	L_c (nm)	L_c/d_{002}	Crystallinity Percentage
BWSC	0.317	0.143	0.451	28.22
BWSAC	0.338	0.162	0.479	31.56

The degree of graphitization of carbonaceous materials can be estimated from the value of the interlayer spacing (d). A greater stacking height (L_c) represents a thicker graphite-like structural layer. Similarly, a higher average carbon layer (L_c/d) further suggests a denser structure (Su *et al.* 2012). The values for interlayer spacing (d) were 0.317 nm and 0.338 nm for BWSC and BWSAC, respectively, similar to the ideal graphite spacing of 0.335 nm (Wenjing and Guangjie 2012). After activation at 700 °C, the value for d decreased but the value for crystallinity, L_c, and L_c/d increased. This implies that the aromatic structure of BWSC was changed to a graphitic structure at approximately 700 °C (Liu and Zhao 2012). A similar trend was observed for activated carbon prepared from liquefied wood after steam activation (Liu and Zhao 2012).

The thermal stability of BWS, BWSC, and BWSAC was investigated using the thermogravimetric method. The thermal degradation curve for all the samples shows several stages. The first degradation step at approximately 70 to 130 °C corresponds to the evaporation of adsorbed water. The second degradation step for BWS proceeds in the temperature range of 200 to 300 °C for hemicellulose and 300 to 400 °C for cellulose. It has been reported that the degradation of hemicelluloses partially overlaps with cellulose degradation in the case of biomass, and lignin degradation proceeds within the temperature range of 200 to 800 °C (Gronli *et al.* 2002; Putun *et al.* 2007). The maximum weight loss of BWS was observed near 365 °C because of the thermal degradation of cellulose. Compared to BWS, BWSC and BWSAC showed higher thermal stability. As the temperature increases, the sample contains a larger proportion of stable carbon particles, which are more heat-resistant. This phenomenon is evident and can be observed from Table 9 and Fig. 8.

The proportion of fixed carbon and ash was higher in BWSC and BWSAC than in BWS. The amount of volatile matter decreased substantially after the activation process, which released gas and liquid products because of the volatilization of organic compounds. The carbon content of the sample increased from 24.50% to 70.90% after activation of the bio-char. This illustrated that prepared biochar after base catalytic activation method was suitable to produce carbonaceous materials competent for adsorbent preparation. Similarly, ultimate analysis revealed that the elemental carbon

content in BWSAC was higher than that in BWSC. The hydrogen content was reduced after the activation process.

Table 9. Proximate and Ultimate Analyses of BWS, BWSC, and BWSAC Samples

Proximate Analysis	**BWS (wt%)**	**BWSC (wt%)**	**BWSAC (wt%)**
Moisture	8.08	5.16	3.05
Volatile Matter	63.34	58.19	19.01
Fixed Carbon	24.50	31.54	70.90
Ash	4.08	5.11	7.04
Ultimate Analysis	**BWS (wt%)**	**BWSC (wt%)**	**BWSAC (wt%)**
Percentage Carbon	45.09	57.05	71.66
Percentage Hydrogen	14.99	13.40	7.51
Percentage Nitrogen	6.33	5.13	1.52
Others	33.59	24.42	19.31

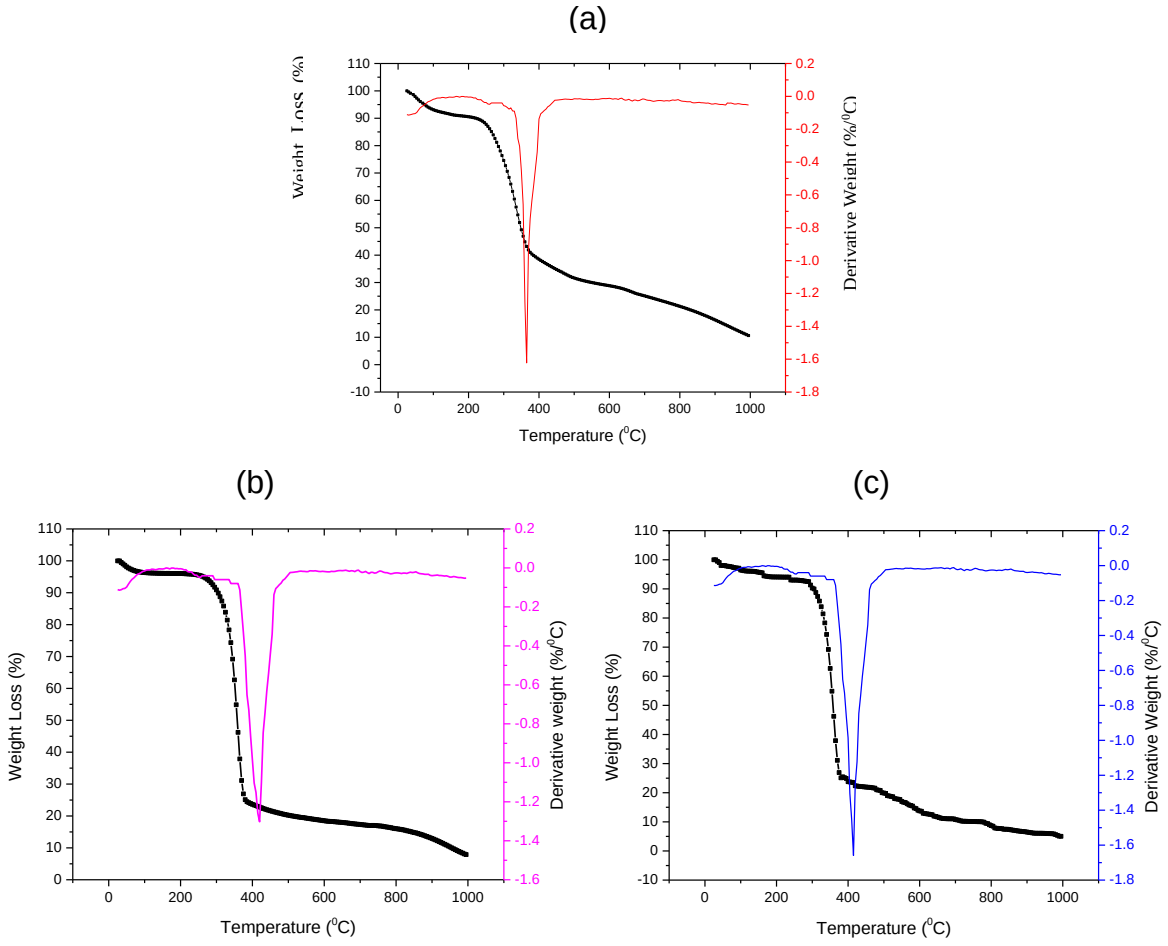

Fig. 8. TGA and DTG profile for (a) BWS, (b) BWSC, and (c) BWSAC

CONCLUSIONS

1. Graphitic phase biochar (BWSAC) with high carbon content and surface area was successfully synthesized from Durian wood sawdust (BWS) using a two-step method that combined microwave-assisted carbonization with subsequent activation in the presence of a base catalytic medium under carbon dioxide gas flow.
2. Microwave- assisted carbonization yielded biochar (BWSC) with low surface area, which was further activated for substantial removal of Pb(II) cations from a single solute system.
3. Thermogravimetric analysis of the mesoporous carbon showed higher thermal stability with less ash content compared with BWS, and BWSC.
4. The optimum removal efficiency of Pb(II) was 91.22%. The experimental conditions at this optimum point were pH = 5.86, C_0 = 57.77 mg/L, and T = 53.85 °C.
5. The fit of the model was checked in terms of determination coefficient (R^2). In this study, the value of the determination coefficient obtained was R^2 = 0.949. Furthermore, the value elucidated for the adjusted determination coefficient (adjusted R^2 = 0.904) was also high, reflecting the significance of the predictive model.

ACKNOWLEDGMENTS

The authors would like to thank Grand Challenge (GC001B-14SBS) and BKP (BK054-2015) of University Malaya, Malaysia for their cordial support in completing this work.

REFERENCES CITED

Azargohar, and Dalai, A. K. (2006). "Biochar as a precursor of activated carbon," *Appl. Biochem. Biotechnol.* 129-132, 762-774. DOI: 10.1385/ABAB:131:1:762

Acharya, J., Sahu, J. N., Sahoo, B. K., Mohanty, C. R., and Meikap, B. C. (2009). "Removal of chromium (VI) from wastewater by activated carbon developed from *Tamarind* wood activated with zinc chloride," *Chem. Eng. J.* 150(1), 25-39. DOI: 10.1016/j.cej.2008.11.035

Amini, M., Habibullah, Y. Nader, B., Ali Akbar, Z. L., Farshid, G., Ali, D., and Mazyar, S. (2008). "Application of response surface methodology for optimization of lead biosorption in an aqueous solution by *Aspergillus*," *J. Hazard. Mater.* 154(1-3), 694-702. DOI: 10.1016/j.jhazmat.2007.10.114

Antal, M. J., Wade, S. R., and Nunoura, T. (2007). "Biocarbon production from Hungarian sunflower shells," *J. Anal. Appl. Pyrol.* 79(1-2), 86-90. DOI: 10.1016/j.jaap.2006.09.005

Adinata, D., Daud, M. A.W., and Aroua, M. K. (2007). "Preparation and characterization of activated carbon from palm shell by chemical activation with K_2CO_3," *Bioresour. Technol.* 98(1), 145-149. DOI:10.1016/j.biortech.2005.11.006

Ahmad, A. A., and Hameed, B. H. (2010). "Effect of preparation conditions of activatedcarbon from bamboo waste for real textile wastewater," *J. Hazard. Mater.* 173(1-3), 487-493. DOI: 10.1016/j.jhazmat.2009.08.111

Ahmad, A. A., Hameed, B. H., and Ahmad, A. L. (2009). "Removal of disperse dye from aqueous solution using waste-derived activated carbon: optimization study," *J. Hazard. Mater.* 170(2-3), 612-619. DOI: 10.1016/j.jhazmat.2009.05.021

Alam, M. Z., Muyibi, S. A., and Toramae, J. (2007). "Statistical optimization of adsorption processes for removal of 2,4-dichlorophenol by activated carbon derived from oil palm empty fruit bunches," *J. Environ. Sci*. 19(6), 674-677. DOI: 10.1016/S1001-0742(07)60113-2

Avramescu, A., Andreescu, S., Noguer, T., Bala, C., Andreescu, D., and Marty, J.-L. (2002). "Biosensors designed for environmental and food quality control based on screen-printed graphite electrodes with different configurations," *Anal. Bioanal. Chem*. 374(1), 25-32. DOI: 10.1007/s00216-002-1312-0

Bulut, Y., and Tez, Z. (2007). "Removal of heavy metals from aqueous solution by sawdust adsorption," *J. Env. Sci.* 19(2), 160-166. DOI: 10.1016/S1001-0742(07)60026-6

Chen, J., Wang, L., and Zou, S. (2007). "Determination of lead biosorption properties by experimental and modeling simulation study," *Chem. Eng. J.* 131(1-3), 209-215. DOI: 10.1016/j.cej.2006.11.012

Chowdhury, Z. Z., Zain, S. M., Khan, R. A., and Khalid, K. (2012a). "Batch and fixed bed adsorption studies of lead(ii) cations from aqueous solutions onto granular activated carbon derived from mangostana garcinia shell," *BioResources* 7(3), 2895-2915. DOI: 10.15376/biores.7.3.2895-2915

Chowdhury, Z. Z., Zain, S. M., Khan, R. A., and Khalid, K. (2012b). "Process variables optimization for preparation and characterization of novel adsorbent from lignocellulosic waste," *BioResources*, 7(3), 3732-3754. DOI: 10.15376/biores.7.3.3732-3754

Chowdhury, Z. Z., Abd Hamid, S. B., Das, R., Hasan, H. R., Zain, S. M., Khalid, K. and Uddin, M. N. (2013). "Preparation of carbonaceous adsorbents from lignocellulosic biomass and their use in removal of contaminants from aqueous solution," *BioResources* 8(4), 6523-6555. DOI:10.15376/biores.8.4.6523-6555

Chowdhury, Z. Z, Hasan, M. R., Abd Hamid, S. B., Samsudin, E. M., Zain, S. M., and Khalid, K. (2015). "Catalytic pretreatment of biochar residues derived from lignocellulosic feedstock for equilibrium studies of manganese, Mn(II) cations from aqueous solution," *RSC Adv.* 5, 6345-6356. DOI: 10.1039/C4RA09709B

Department of Agriculture, Malaysia, http://www.doa. Gov.my/statistik/buah03-08.html, accessed on 23rd April 2009.

Daniel, M., Francisco, C., Esteve M.-F., and Salvador, A. (1997). "Determination of organophosphorus and carbamate pesticides using a biosensor based on a polishable, 7,7,8,8-tetracyanoquino-dimethane-modified, graphite-epoxy biocomposite," *Anal. Chim. Acta*, 337(3), 305-313. DOI: 10.1016/S0003-2670(96)00384-4

Feng, Q., Lin, Q., Gong, F., Sugita, S., and Shoya, M. (2004). "Adsorption of lead and mercury by rice husk ash," *J. Colloid Interf. Sci.* 278(1), 1-8. DOI: 10.1016/j.jcis.2004.05.030

Funke, A., and Ziegler, F. (2010). "Hydrothermal carbonization of biomass: a summary and discussion of chemical mechanisms for process engineering," *Biofuels Bioprod. Biorefin.* 4(2), 160-177. DOI: 10.1002/bbb.198

Gronli, M. G., Varhegyi, G., and Diblasi, C. (2002). "Thermogravimetric analysis and devolatilization kinetics of wood," *Ind. Eng. Chem. Res*. 41(17), 4201-4208. DOI: 10.1021/ie0201157

Gunaraj, V., and Murugan, N. (1999). "Application of response surface methodologies for predicting Weld base quality in submerged arc welding of pipes," *J. Mater. Process Technol.* 88 (1-3), 266-275. DOI: 10.1016/S0924-0136(98)00405-1

Han, Y., Boateng, A. A., Qi, P. X., Lima, I. M., and Chang, J. (2013). "Heavy metal and phenol adsorptive properties of biochars from pyrolyzed switchgrass and woody biomass in correlation with surface properties," *J. Env. Manag.* 118, 196-204. DOI: 10.1016/j.jenvman.2013.01.001

Holan, Z. R., and Volesky, B. (1994). "Biosorption of Pb and Ni by biomass of marine algae," *Biotechnol. Bioeng.* 43(1), 1001-1009. DOI: 10.1002/bit.260431102

Vieira, I. C., and Fatibello-Filho, O. (2000). "Biosensor based on paraffin/graphite modified with sweet potato tissue for the determination of hydroquinone in cosmetic cream in organic phase," *Talanta* 52(4), 681-689.

Jamari, S. S., and Howse, J. R. (2012). "The effect of the hydrothermal carbonization process on palm oil empty fruit bunch," *Biomass Bioenerg.* 47, 82-90. DOI: 10.1016/j.biombioe.2012.09.061

Johari, I. S., Yusof, N. S., Haron, J., and Mohd Nor, S. M. (2013). "Preparation and characterization of poly(ethyl hydrazide)-grafted oil palm empty fruit bunch fibre for the removal of Cu(II) ions from an aqueous environment," *Molecules* 18, 8461-8472. DOI: 10.3390/molecules18078461

Jalali, R., Ghafourian, H., Asef, Y., Davarpanah, S. J., and Sepehr, S. (2002). "Removal and recovery of lead using nonliving biomass of marine algae," *J. Hazard Mater.* 92 (3), 253-262. DOI: 10.1016/S0304-3894(02)00021-3

Jun, T. Y., Arumugam, S. D., Abdul Latip, N. H., Abdullah, A. M., and Latif, P. A. (2010). "Effect of activation temperature and heating duration on physical characteristics of activated carbon prepared from agriculture waste," *Environ. Asia* 3, 143-148.

Kobayashi, H., Kaiki, H., Shrotri, A., Techikawara, K., and Fukuoka, A. (2016). "Hydrolysis of woody biomass by a biomass-derived reusable heterogeneous catalyst," *Chemical Science* 7(1), 692-696, DOI: 10.1039/c5sc03377b.

Liu, Z., and Zhang, F. S. (2009). "Removal of lead from water using biochars prepared from hydrothermal liquefaction of biomass," *J. Hazard Mater.* 167(1-3), 933-939. DOI: 10.1016/j.jhazmat.2009.01.085

Lo, W., Chua, H., Lam, K. H., and Bi, S. H. (1999). "A comparative investigation on the biosorption of lead by filamentous fungal biomass," *Chemosphere* 39(15), 2723-2736. DOI: 10.1016/S0045-6535(99)00206-4

Lu, J., Drzal, L. T., Worden, R. M., and Lee, I. (2007). "Simple fabrication of a highly sensitive glucose biosensor using enzymes immobilized in exfoliated graphite nanoplatelets nafion membrane," *Chem. Mater*. 19(25), 6240-6246.

Montgomery, D.C. (2001). *Design and Analysis of Experiments*, 5th Ed., John Wiley and Sons, New York, NY.

Munusamy, K., Rajesh, S. and Bajaj, H. C. (2011). "Tamarind seed carbon: Preparation and methane uptake," *BioResources* 6(1), 537-551. DOI: 10.15376/biores.6.1.537-551

Mohan, D., Sarswat, A., Ok, Y. S., and Pittman Jr., C. U. (2014). "Organic and inorganic contaminants removal from water with biochar, a renewable, low cost and sustainable

adsorbent-A critical review," *Bioresour Technol*. 160, 191-202. DOI: 10.1016/j.biortech.2014.01.120

Pavan Flávio, A., Mazzocato, A. C., Jacques Rosângela, A., and Diassilvio, P. (2008). "Ponkan peel: A potential biosorbent for removal of Pb(II) ions from aqueous solution," *Biochem. Eng. J.* 40 (2), 357-362. DOI: 10.1016/j.bej.2008.01.004

Putun, E., Uzun, B. B., and Putun, A. E. (2007). "Composition of products obtained via fast pyrolysis of olive-oil residue: effect of pyrolysis temperature," *J. Anal. Appl. Pyrol.* 79(1-2), 147-153. DOI: 10.1016/j.jaap.2006.12.005

Sahu, J. N, Acharya, J., and Meikap, B. C. (2009a). "Response surface modeling and optimization of chromium(vi) removal from aqueous solution using tamarind wood activated carbon in batch process," *J. Hazard Mater.*172(2) , 818-825. DOI:10.1016/j.jhazmat.2009.07.075

Sahu, J. N., Agarwal, S., Meikap, B. C. and Biswas, M. N. (2009b). "Performance of a modified multi-stage bubble column reactor for lead(ii) and biological oxygen demand removal from waste water using activated rice husk," *J. Hazard. Mater.* 161(1), 317-324. DOI: 10.1016/j.jhazmat.2008.03.094

Sathish-Kumar, K., Vázquez-Huerta, G., Andrés Rodríguez-Castellanos, H., Poggi-Varaldo, M., and Solorza-Ferial, O. (2012). "Microwave assisted synthesis and characterizations of decorated activated carbon," *Int. J. Electrochem. Sci.* 7, 5484-5494.

Selatnia, A., Boukazoula, N., Kchid, N., Bakhti, M. Z., Chergui, A., and Kerchich, Y. (2004). "Biosorption of lead(II) from aqueous solution by a bacterial dead *streptomyces rimosus* biomass," *Biochem. Eng. J.* 19(2), 127-135. DOI: 10.1016/j.bej.2003.12.007

Singanan, M., and Peters, E. (2013). "Removal of toxic heavy metals from synthetic wastewater using a novel biocarbon technology," *J. Env. Chem. Eng.* 1(4), 884-890. DOI: 10.1016/j.jece.2013.07.030

Singh, C. K., Sahu, J. N., Mahalik, K. K., Mohanty, C. R, Rajmohan, B. and Meikap, B. C. (2008). "Studies on the removal of Pb(II) fromwastewater by activated carbon developed from tamarind wood activated with sulphuric acid,"*J. Hazard Mater.* 153(1-3), 221-228. DOI:10.1016/j.jhazmat.2007.08.043

Srinivasakannan, C., and Bakar, M. Z. A. (2004). "Production of activated carbon from rubber wood sawdust," *Biomass Bioenerg.* 27(1), 89-96. DOI: 10.1016/j.biombioe.2003.11.002

Su, C., Zeng, Z., Peng, C., and Lu, C. (2012). "Effect of temperature and activators on the characteristics of activated carbon fibers prepared from viscose-rayon knitted fabrics," *Fibers and Polymers* 13(1), 21-27. DOI: 10.1007/s12221-012-0021-3

Tay, J. H, Chen, X. J., Jeyaseelan, S., and Graham, N. (2001). "Optimising the preparation of activated carbon from digested sewage sludge and coconut husk," *Chemosphere* 44(1), 45-51. DOI: 10.1016/S0045-6535(00)00383-0

Tangjuank, S., Insuk, N., Udeye, V., and Tontrakoon, J. (2009). "Chromium (III) sorption from aqueous solutions using activated carbon prepared from cashew nut shells," *Int. J. Phys. Sci.* 4(8), 412-417.

Ucun, H., Bayhan, Y. K.,Kaya, Y., and Algur, O. F. (2002). "Biosorption of chromium(VI) from aqueous solution by cone biomass of *Pinus sylvestris*," *Bioresour. Technol.* 85(2), 155-158. DOI: 10.1016/S0960-8524(02)00086-X

Veglio, F., and Beolchini, F. (1997). "Removal of metals by biosorption: A review," *Hydrometallurgy* 44(3), 301-316. DOI: 10.1016/S0304-386X (96)00059-X

Volesky, B., May, H., and Holan, Z. R. (1992). "Cadmium biosorption by *Saccharomyces cerevisiae*," *Biotechnol. Bioenerg.* 41(8), 826-829. DOI: 10.1002/bit.260410809

Wang, S. and Zhu, Z. H. (2007). "Effects of acidic treatment of activated carbons on dye adsorption," *Dyes and Pigments* 75(2), 306-314. DOI: 10.1016/j.dyepig.2006.06.005

Wenjing, L., and Guangjie, Z. (2012). "Effect of temperature and time on microstructure and surface functional groups of activated carbon fibers prepared from liquefied wood," *BioResources* 7(4), 5552-5567. DOI: 10.15376/biores.7.4.5552-5567

Yan, G., and Viraraghavan, T. (2003). "Heavy-metal removal from aqueous solution by fungus *Mucor rouxii*," *Water Res.* 37(18) 4486-4496. DOI: 10.1016/S0043-1354(03)00409-3

Zhang, Y., Yang, S., Jian-Quan, W., Tong-Qi, Y., and Sun, R. (2014). "Preparation and characterization of lignocellulosic oil sorbent by hydrothermal treatment of *Populus* fiber", *Materials* 7, 6733-6747. DOI: 10.3390/ma7096733

Zhu, W., Zhou, K., Li, H. X., Wang, H. F., and Iang, J. P. (2013). "One-pot growth of free-standing cnts/TiO_2 nanofiber membrane for enhanced photocatalysis," *Mater Lett.* 95, 13-16. DOI: 10.1016/j.matlet.2013.01.004

Article submitted: August 24, 2015; Peer review completed: December 18, 2015; Revised version received: February 15, 2016; Accepted: February 17, 2016; Published: March 1, 2016.
DOI: 10.15376/biores.11.2.3637-3659